

# Mechanical properties and microstructure of $\beta$ -SiAlON– $\beta$ -SiC composites by pressureless sintering

C. YAMAGISHI, K. TSUKAMOTO, J. HAKOSHIMA, H. SHIMOJIMA,  
Y. AKIYAMA

Central Research Laboratory, Nihon Cement Co. Ltd, 1-2-23 Kiyosumi, Koutouku, Tokyo 135,  
Japan

$\beta$ -SiAlON– $\beta$ -SiC composites containing up to 12 wt%  $\beta$ -SiC were prepared by pressureless sintering. The strength of composites at room temperature remained relatively unchanged, whereas strength at 1200 °C increased for composites. The fracture toughness ( $K_{Ic}$ ) for composites was higher than that for  $\beta$ -SiAlON ceramics. The maximum value was 5.4 MPa m<sup>1/2</sup> for 6 wt%  $\beta$ -SiC, and this was an improvement of 15% in comparison with  $\beta$ -SiAlON ceramics. From SEM observations, an improvement in  $K_{Ic}$  values was attributed to crack deflections and branching-off of cracks. Intra-granular fractures were frequently observed in  $\beta$ -SiAlON. From TEM observations,  $\beta$ -SiAlON crystals were nanocomposites, within which existed the fine crystals in  $\beta$ -SiAlON crystal. For composite,  $\beta$ -SiAlON and  $\beta$ -SiC crystals were directly in contact. The mismatching zone was observed in  $\beta$ -SiC.

## 1. Introduction

$\beta$ -SiAlON [1–3] ceramics ( $\text{Si}_{6-z}\text{Al}_z\text{O}_z\text{N}_{8-z}$ ,  $z = 0\text{--}4.2$ ) have received considerable interest in recent years for engine and gas-turbine applications, due to their high-temperature strength, oxidation resistance, chemical stability and low thermal expansion coefficient.

In the past,  $\beta$ -SiAlON was synthesized from  $\text{Si}_3\text{N}_4$ ,  $\text{Al}_2\text{O}_3$  and AlN powders by reaction bonding using hot pressing [4, 5]. However, the sintered body was not uniform because these powders were not mixed uniformly. Therefore abnormal grain growth occurred and the mechanical properties were unsatisfactory for applications. To improve the mechanical properties, combining these materials with other ceramics by hot pressing or gas pressure sintering was investigated [6, 7].  $\beta$ -SiAlON and  $\beta$ -SiAlON– $\beta$ -SiC composites were prepared by pressureless sintering using high-purity and fine  $\beta$ -SiAlON powders synthesized by carbo-thermal reduction [8].

This paper describes the mechanical properties and microstructure of  $\beta$ -SiAlON– $\beta$ -SiC composites prepared by pressureless sintering.

## 2. Experimental procedure

### 2.1. Preparation of $\beta$ -SiAlON– $\beta$ -SiC composites

$\beta$ -SiAlON powder,  $z = 0.5$  ( $\text{Si}_{5.5}\text{Al}_{0.5}\text{O}_{0.5}\text{N}_{7.5}$ ), was prepared by carbo-thermal reduction at 1450 °C for 5 h in  $\text{N}_2$  atmosphere. Raw materials were high-purity  $\text{SiO}_2$  powder, carbon powder and aluminium hydroxide which was prepared by hydrolysis of aluminium

isopropoxide. Commercial  $\beta$ -SiC powder (medium grain size ranged between 0.2 and 0.3  $\mu\text{m}$ ) and commercial  $\text{Y}_2\text{O}_3$  were mixed with the  $\beta$ -SiAlON powder. The additional amounts of  $\beta$ -SiC were 0, 3, 6, 9 and 12 wt%, and of  $\text{Y}_2\text{O}_3$ , 5 wt% for  $\beta$ -SiAlON.

Composite powder was made by milling 100 g of the above-mentioned powder with 250 ml of ethanol for 24 h using a pot mill with silicon nitride ( $\text{Si}_3\text{N}_4$ ) beads, then drying under diminished pressure. Medium grain sizes of composite powders were ranged between 0.3 and 0.5  $\mu\text{m}$ , measured with a sedigraph. Each composite powder was formed into green bodies 50 mm dia.  $\times$  5 mm thick under 33 MPa and cold isostatic pressing at 98 MPa. These green bodies were sintered in a carbon crucible at 1780 °C for 3 h under  $\text{N}_2$  atmosphere by pressureless sintering.  $\beta$ -SiAlON and  $\beta$ -SiAlON– $\beta$ -SiC composites were obtained.

### 2.2. Measurement of mechanical properties

Samples were machined from sintered bodies to test bars, 40 mm long, 4 mm wide and 3 mm thick. The strength of the samples was measured by three-point bending; the span was 30 mm and the cross-head speed 0.5 mm min<sup>-1</sup>. Bending strength was measured at room temperature ( $n = 5$ ) and at 1200 °C ( $n = 3$ ) in air. Fracture toughness ( $K_{Ic}$ ) was measured by Vickers indenter with 20 kg weight, 30 s loading time (indentation fracture (IF) method). Fracture toughness ( $K_{Ic}$ ) was calculated using Equation 1 [9]. Elastic modulus was measured by pulse-echo testing using a

test bar 40 mm long, 4 mm wide and 3 mm thick.

$$K_{1c} = \frac{0.026 \times E^{2/1} \times P^{2/1} \times a}{C^{3/2}} \quad (\text{Pa m}^{1/2}) \quad (1)$$

where  $E$  is the elastic modulus (Pa);  $C$  is the radius of the medium crack (m);  $P$  is the load (N); and  $a$  is the length of the half-diagonal of indent (m).

### 2.3. Crystalline phase and microstructure observations

The crystalline phases of the sintered body were determined by X-ray diffraction (XRD). Crack propagation and microstructure of the sintered body were observed using the scanning electron microscope (SEM). The crystalline grains in the composites were observed using the transmission electron microscope (TEM) and energy dispersion X-ray analysis (EDX).

## 3. Results and discussion

### 3.1. Mechanical properties

#### 3.1.1. Relative density and XRD patterns

The relative density of 99% remained unchanged for composites containing up to 9 wt %  $\beta$ -SiC, and a relative density of 98.5% was obtained for 12 wt %  $\beta$ -SiC content. High-density sintered bodies were obtained. Only  $\beta$ -SiAlON and  $\beta$ -SiC crystalline phases were observed in XRD patterns of  $\beta$ -SiAlON- $\beta$ -SiC composites.

#### 3.1.2. Strength

Fig. 1 shows the bending strength of  $\beta$ -SiAlON- $\beta$ -SiC composites at room temperature and at 1200 °C. At room temperature, strength remained relatively unchanged for composites containing up to 12 wt %  $\beta$ -SiC, values being about 800 MPa. At 1200 °C, strength increased for composites containing up to 9 wt %  $\beta$ -SiC content. For 9 wt %  $\beta$ -SiC, strength increased by 12%, as compared with  $\beta$ -SiAlON ceramics (490 MPa), to about 560 MPa.

From the results mentioned above, for specimens having a relative density of more than 98 %,  $\beta$ -SiAlON containing  $\beta$ -SiC had no effect on the increase in strength at room temperature. However,  $\beta$ -SiAlON containing  $\beta$ -SiC contributed to increased strength at 1200 °C.

#### 3.1.3. Fracture toughness

Fig. 2 shows fracture toughness,  $K_{1c}$ , for  $\beta$ -SiAlON- $\beta$ -SiC composites measured by Vickers indenter. Fracture toughness values increased for composites containing up to 6 wt %  $\beta$ -SiC, and then decreased as the  $\beta$ -SiC content increased. Fracture toughness for composites containing up to 12 wt %  $\beta$ -SiC was higher than that for  $\beta$ -SiAlON ceramics. The maximum value was increased by 15 % to 5.4 MPa m<sup>1/2</sup> at 6 wt %  $\beta$ -SiC content in comparison with  $\beta$ -SiAlON ceramics (at 4.7 MPa m<sup>1/2</sup>). Fracture toughness was maximum for composites containing 6 wt %  $\beta$ -SiC,

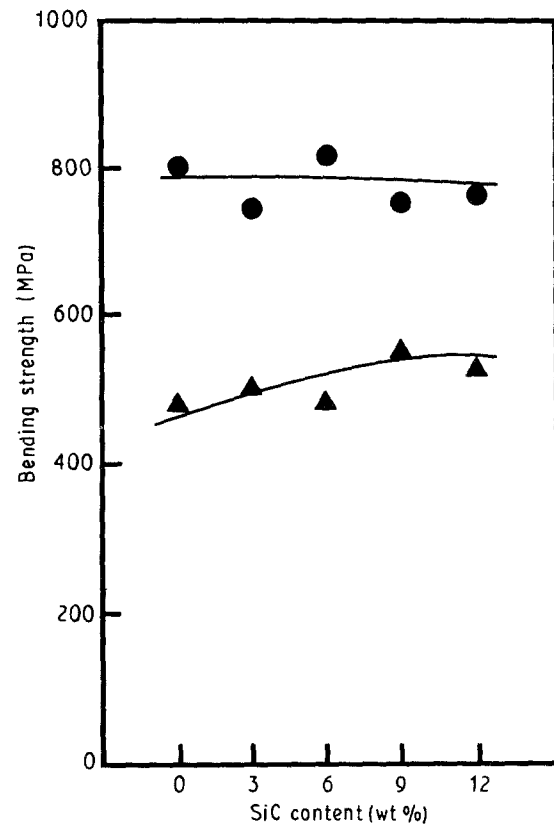


Figure 1 Bending strength of  $\beta$ -SiAlON- $\beta$ -SiC composites at ●, room temperature and ▲, 1200 °C.

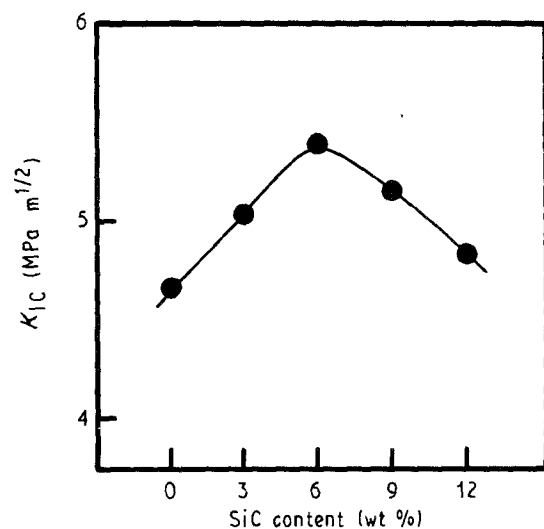


Figure 2 Fracture toughness of  $\beta$ -SiAlON- $\beta$ -SiC composites.

when relative densities were about 100%. Fracture toughness decreased with decreasing relative density.

The strength and fracture toughness for composites up to 12 wt %  $\beta$ -SiC were higher than for  $\beta$ -SiAlON ceramics. Mechanical properties were improved with increasing  $\beta$ -SiC (up to 9 wt %), when the composites for full density were obtained (> 99% R.D.). This means that the  $\beta$ -SiAlON- $\beta$ -SiC composite is very useful for high-temperature materials, where the relative density is about 100%.

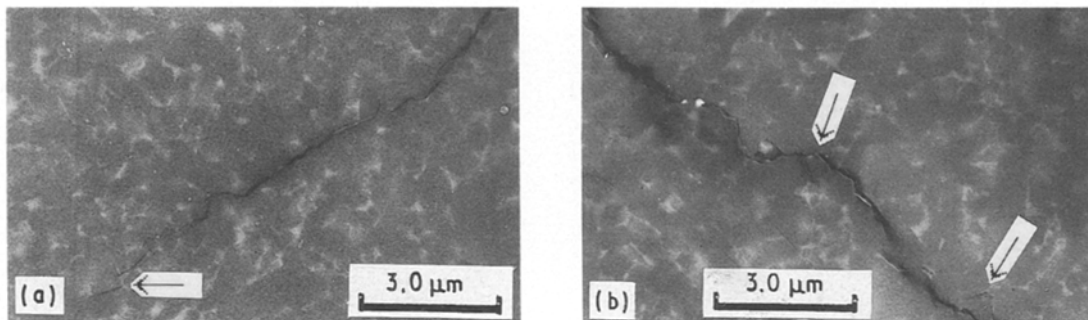


Figure 3 SEM image for polished and indented surfaces of sintered bodies. (a)  $\beta$ -SiAlON ceramics; (b)  $\beta$ -SiAlON- $\beta$ -SiC composites (containing 6 wt %  $\beta$ -SiC).

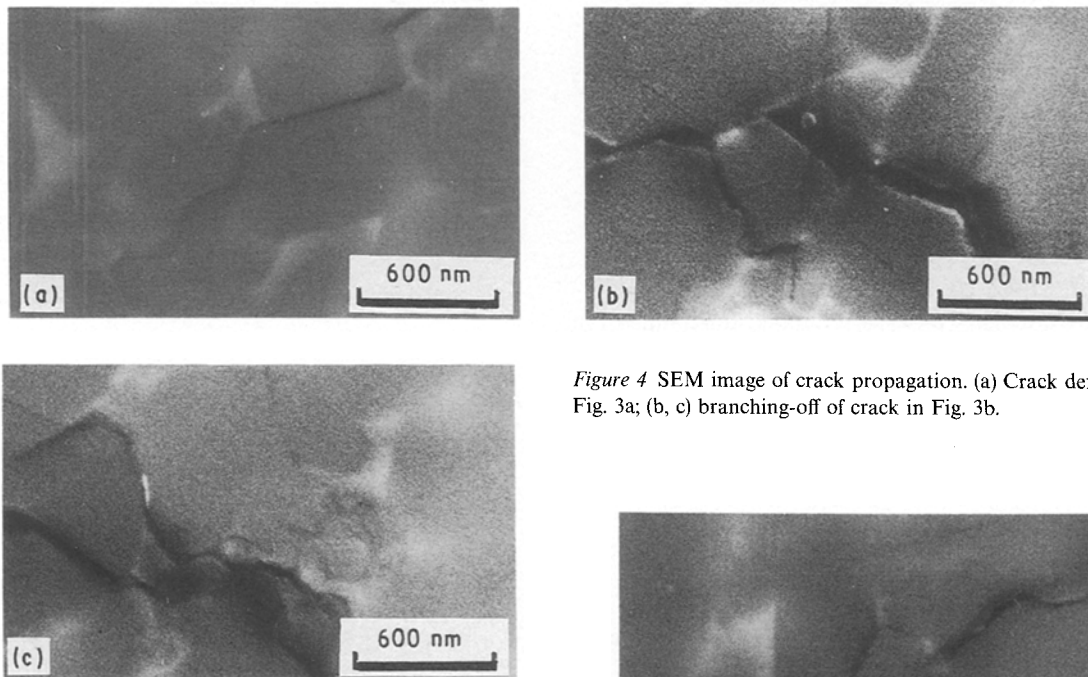


Figure 4 SEM image of crack propagation. (a) Crack deflection in Fig. 3a; (b, c) branching-off of crack in Fig. 3b.

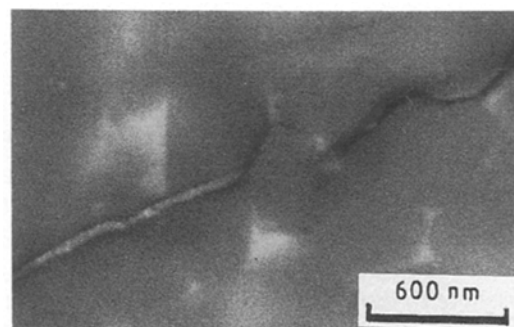


Figure 5 SEM image of intra-granular fracture.

## 3.2. Microstructural observations

### 3.2.1. SEM observations

Fig. 3 shows SEM images of crack propagation for sintered bodies. Fig. 3a is  $\beta$ -SiAlON, and Fig. 3b is the  $\beta$ -SiAlON- $\beta$ -SiC composite containing 6 wt %  $\beta$ -SiC. As shown in Fig. 3,  $\beta$ -SiAlON ceramics have two types of crystalline grains: one is uniaxial, the other prismatic. However the grain growth of the prismatic grain did not proceed as compared with typical silicon-nitride ( $\text{Si}_3\text{N}_4$ ) ceramics.

The crack propagated in deflecting through  $\beta$ -SiAlON ceramics, on the other hand, in deflecting and branching through the composite. Fig. 4a shows crack deflection in  $\beta$ -SiAlON ceramics (arrow in Fig. 3a). Fig. 4b and c shows branching-off of cracks in the composite (arrows in Fig. 3b). It seems that the increasing fracture toughness in  $\beta$ -SiAlON- $\beta$ -SiC composites is attributed to these combined effects (crack deflections and branching-off of cracks).

When  $\beta$ -SiC particles were dispersed in the  $\beta$ -SiAlON matrix, tensile stress occurred at the grain boundaries between  $\beta$ -SiC and  $\beta$ -SiAlON after sintering, because thermal expansion of  $\beta$ -SiC is different from that of  $\beta$ -SiAlON. It seems that crack deflec-

tion and branching-off of cracks result from the residual stress.

In the case of silicon-nitride ceramics, pulling out was observed [10]; however, in the case of  $\beta$ -SiAlON ceramics and  $\beta$ -SiAlON- $\beta$ -SiC composites, cracks cut the grains (see Fig. 5). In particular, these intra-granular fractures were frequently observed in prismatic grains, when the crack propagated vertical to the side of the longer axis on the prismatic grain.

### 3.2.2. TEM observations

$\beta$ -SiAlON ceramics were observed by TEM. Fig. 6 shows  $\beta$ -SiAlON crystals in the ceramics, and Fig. 7 shows the observed results inside the  $\beta$ -SiAlON crystal.  $\beta$ -SiAlON crystals in the sintered body were nanocomposites, which existed as fine crystals ( $< 80$  nm; arrows in Figs 6 and 7) in the  $\beta$ -SiAlON crystal. The

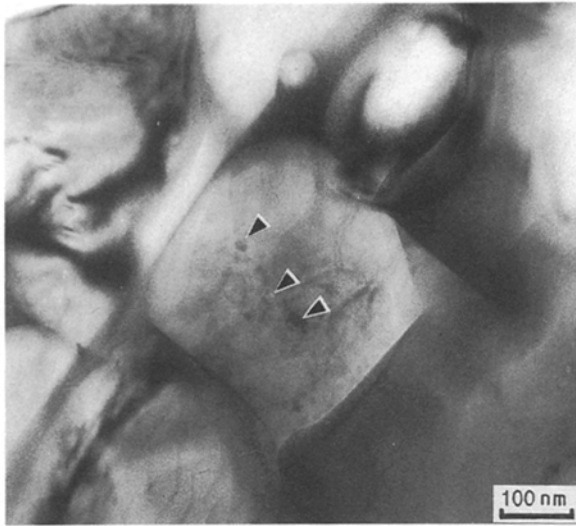


Figure 6 TEM image of  $\beta$ -SiAlON crystals.

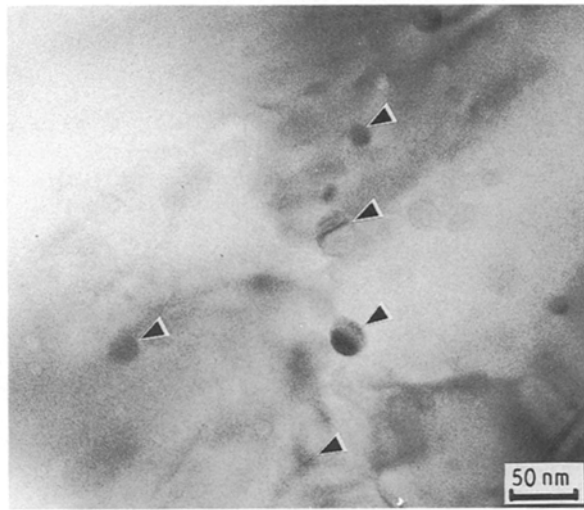


Figure 7 TEM image of  $\beta$ -SiAlON nanocomposite.

nanocomposites were observed in  $\text{Si}_3\text{N}_4$ -SiC composite sintered by the powder synthesized from hexamethyl-disilazane [11]. It seems that the occurrence of  $\beta$ -SiAlON nanocomposites may be attributed to the synthetic process of the  $\beta$ -SiAlON powder.

It is thought that the fine crystals in the  $\beta$ -SiAlON crystal are  $\beta$ -SiC crystals, in consideration of the synthetic process of  $\beta$ -SiAlON powder and ceramics. The modulations were observed inside  $\beta$ -SiAlON crystals. It seems that the modulations are attributed to strain, which results from the difference between the thermal expansion of  $\beta$ -SiAlON and  $\beta$ -SiC crystals. The  $\beta$ -SiAlON- $\beta$ -SiC composite was observed by TEM (Fig. 8). Fig. 8 also shows diffraction patterns of the  $\beta$ -SiAlON- $\beta$ -SiC composite observed by TEM. The results of EDX analysis, (a) and (b) in Fig. 8, are shown in Fig. 9. The stacking fault was observed in crystal (a) along the  $c$ -axis. The atoms regularly arranged in crystal (b), as shown in Fig. 8. The silicon was detected in crystal (a), but on the other hand silicon,

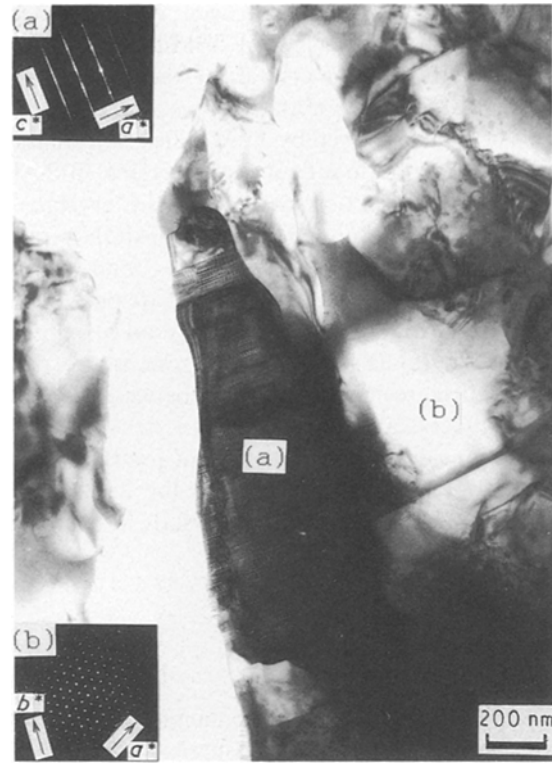


Figure 8 TEM image of  $\beta$ -SiAlON- $\beta$ -SiC composite and diffraction patterns of each crystal.

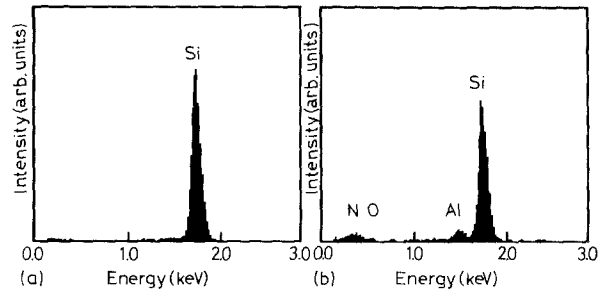


Figure 9 Spectrum of spot analysis (a) of (a) in Fig. 8; (b) of (b) in Fig. 8.

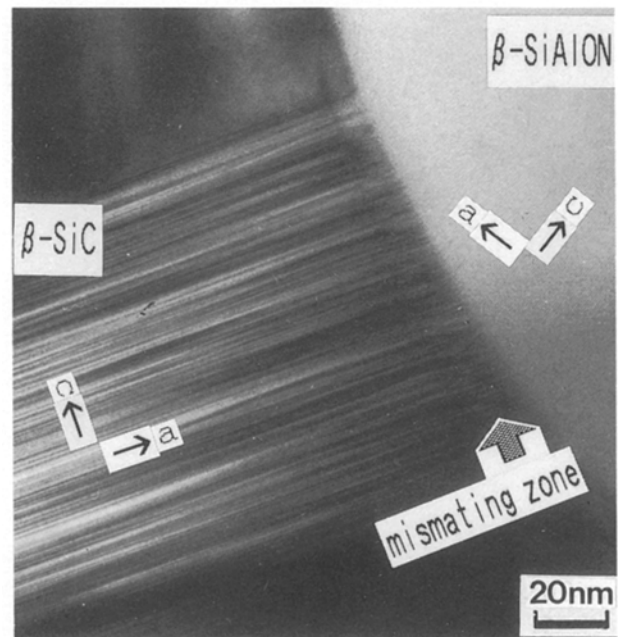


Figure 10 TEM image of the interface between  $\beta$ -SiAlON and  $\beta$ -SiC.

aluminium, oxygen and nitrogen were detected in crystal (b). From the results of TEM and EDX, crystal (a) was  $\beta$ -SiC, and the crystal (b) was  $\beta$ -SiAlON.

Fig. 10 shows the interface between  $\beta$ -SiAlON and  $\beta$ -SiC crystals observed by TEM. The grain-boundary phases were not found at the interface.  $\beta$ -SiAlON crystal was in direct contact with  $\beta$ -SiC crystal.

At the interface, the atoms in  $\beta$ -SiAlON regularly arranged without influence of the bond to  $\beta$ -SiC crystal. However, the 100–150 nm of  $d$ -space mismatching zone around the  $\beta$ -SiAlON crystal was observed in  $\beta$ -SiC crystal. It seems that the zone is a relaxation layer of disagreement of lattices between  $\beta$ -SiAlON and  $\beta$ -SiC crystals.

It is considered that one reason for the improvement of mechanical properties is the interface state between  $\beta$ -SiAlON and  $\beta$ -SiC crystals in composites.

#### 4. Conclusions

$\beta$ -SiAlON- $\beta$ -SiC composites containing up to 12 wt %  $\beta$ -SiC were prepared by pressureless sintering. The mechanical properties and microstructure of the composites were investigated. The results obtained were as follows.

1. The strength at room temperature of about 800 MPa remained relatively unchanged. The strength at 1200 °C increased for composites containing up to 9 wt %  $\beta$ -SiC. The maximum value was 560 MPa.

2. The fracture toughness for composites was higher than that for  $\beta$ -SiAlON ceramics. The maximum value was 5.4 MPa m<sup>1/2</sup> for 6 wt %  $\beta$ -SiC, an improvement by 15% in comparison with  $\beta$ -SiAlON ceramics. From SEM observations, the improvement in fracture toughness values for composites was

attributed to crack deflections and branching-off of cracks.

3. Intra-granular fractures were frequently observed in  $\beta$ -SiAlON. It is suggested that the crack propagation behaviour of  $\beta$ -SiAlON and Si<sub>3</sub>N<sub>4</sub> is different.

4. From TEM observations,  $\beta$ -SiAlON crystals were nanocomposites which existed as fine crystals in  $\beta$ -SiAlON crystals.

5. For the composite, the grain-boundary phases were not found at the interfaces between  $\beta$ -SiAlON and  $\beta$ -SiC crystals, thus  $\beta$ -SiAlON and  $\beta$ -SiC crystals were in direct contact. The mismatching zone was observed in  $\beta$ -SiC crystals.

#### References

1. K. H. JACK, *J. Mater. Sci.* **11** (1976) 1135.
2. Y. OYAMA, *Jpn J. Appl. Phys.* **11** (1972) 760.
3. Y. OYAMA and S. KAMIGAITO, *Yohyo-Kyoukai-Shi* **80** (1972) 327.
4. K. KOBAYASHI, S. UMEBAYASHI and K. KISHI, *ibid.* **89** (1981) 550.
5. S. UMEBAYASHI, K. KISHI, E. TANI and K. KOBAYASHI, *ibid.* **92** (1984) 35.
6. H. NAKAMURA, S. UMEBAYASHI and K. KISHI, *Ceram. Soc. Jpn* **98** (1990) 243.
7. K. KISHI, S. UMEBAYASHI, E. TANI, K. KOBAYASHI and H. NAKAMURA, *Yohyo-Kyoukai-Shi* **95** (1987) 450.
8. K. TSUKAMOTO, C. YAMAGISHI, J. HAKOSHIMA and Y. AKIYAMA, *Amer Ceram. Soc. 92nd annual meeting*, **83** (1990) S IV-90.
9. B. R. LAWN and A. G. EVANS, *J. Amer. Ceram. Soc.* **63** (1980) 574.
10. F. F. LANGE, *ibid.* **62** (1979) 428.
11. K. NIIHARA, T. HIRANO, A. NAKAHIRA, K. OJIMA, K. IZAKI and T. KAWAKAMI, *Materials Research Society, International Meeting on Advanced Materials Tokyo* (1988) p. 107.

Received 10 December 1990  
and accepted 13 May 1991